Magnetic diffuse scattering and the triple-Q structure in FCC γ-MnNi

1990 J. Phys.: Condens. Matter 2 6013

(http://iopscience.iop.org/0953-8984/2/27/008)

J. Phys.: Condens. Matter 2 (1990) 6013–6030. Printed in the UK

Magnetic diffuse scattering and the triple-Q structure in FCC γ-MnNi

M W Long† and O Moze‡§

† School of Physics, Bath University, Claverton Down, Bath BA2 7AY, UK
‡ Istituto MASPEC del CNR, Via Chiavari 18/A, 43100, Parma, Italy
§ Istituto ISRN del CNR, Via E Fermi 38, 00044, Frascati, Roma, Italy

Received 27 June 1989, in final form 5 October 1989

Abstract. The magnetic diffuse scattering from cubic alloys of γ-MnNi is very difficult to explain using a collinear model for the spin structure without introducing physically unjustifiable spin distortions. We show how to generate the experimentally observed scattering with a parameter free model based on short range Heisenberg interactions between spins in a triple-Q ground state. We do however require short range phase coherence between neighbouring impurities in order to be able to explain the high diffuse intensity.

1. Introduction

There has been a great deal of both experimental and theoretical work concerning the nature of the magnetic structure of γ-Mn based alloys [1–11]. For a long time the magnetic structure of the γ-Mn alloys has been assumed to be the collinear type I antiferromagnet, consisting of ferromagnetic sheets perpendicular to the (001) direction with the spins aligned along (001) (figure 1(a)), thus having tetragonal symmetry. The FCC lattice is magnetically *frustrated*, however, and this means that there are other possible spin arrangements to be considered.

The simplest understanding of topological frustration is achieved by considering an equilateral triangle of spins. If any two of the spins are aligned antiparallel, then the third spin cannot be made simultaneously antiparallel to both, and so this third spin is frustrated and unable to decide where to point. The face centre cubic lattice has many equilateral triangles and so many spins are frustrated. A more quantitative measure of frustration is to study the degeneracy of the minimum of the structure factor [11]. The relevant degeneracy for type I antiferromagnets constitutes the triply degenerate points, $\boldsymbol{Q}_1 = (2\pi/a)(1, 0, 0)$, $\boldsymbol{Q}_2 = (2\pi/a)(0, 1, 0)$ and $\boldsymbol{Q}_3 = (2\pi/a)(0, 0, 1)$. The cubic symmetry ensures that if they constitute the minimum, then the minimum is at least triply degenerate, whatever the range of the interaction. We will restrict attention to nearest neighbour interactions in this article, for which the degeneracy is much higher.

As well as the collinear antiferromagnet, another postulated spin structure is the so-called triple-Q structure (figure 1(b)) which has cubic symmetry and as such is a more natural candidate for describing the truly cubic alloys. In fact it is quite easy to categorise *all* the possible type I antiferromagnetic spin configurations [1] and a simple picture emerges with the more exotic states being described as a linear superposition of the three collinear arrangements associated with the three cartesian directions. Each cartesian

0953-8984/90/276013 + 18 $03.50

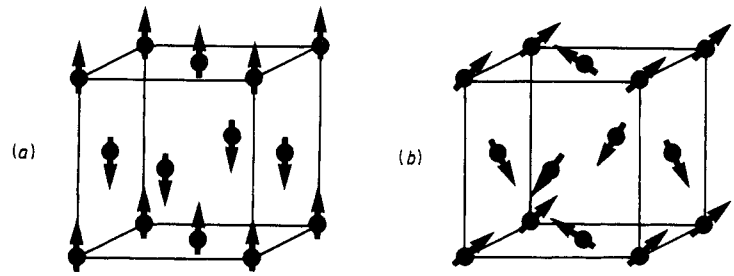

Figure 1. (*a*) The collinear single-Q state: $Q = (2\pi/a)(0,0,1)$. (*b*) The triple-Q state.

direction is associated with a 'Q' and then the collinear phase may be considered a single-Q state whilst the triple-Q state may be considered as a linear superposition of three equal amplitude single-Q states.

A good deal of theoretical work has been carried out in order to examine the relative stability of the single-Q and triple-Q structures. In the first instance, band structure calculations of γ-Mn, assuming the single-Q structure, gave a self-consistent magnetic moment of 1.9 μ_B for Mn [2, 3]. This is smaller than the experimentally determined value of 2.2 μ_B. Also, Fermi surface electron and hole nesting was found and it was argued that such a nesting could give rise to a coupling favouring a multiple-Q structure [4]. The triple-Q state was also found to be relatively stable to the single-Q state by considering a 4-spin exchange interaction [5–8] which removes the degeneracy between single-Q and multi-Q structures, in particular when the electron band is almost half full. A local spin density functional theory has also been used to calculate the relative stability of spin directions in certain types of non-collinear antiferromagnets [9].

The basic phenomena proposed in these theoretical papers are all intrinsic to the ground state. Recently, however, a new suggestion has been put forward [10]. Atomic impurities tend to stabilise different spin arrangements, giving rise to either multiple-Q or single-Q (collinear) structures. A model has recently been proposed whereby it is suggested that γ-Mn is driven from a collinear to a non-collinear structure by doping with, e.g., Ni or Fe [11]. This model proposes a magnetic moment distribution for Mn atoms in the nearest neighbour environment of the paramagnetic transition metal impurity and takes into account the relaxation of the direction of Mn magnetic moments as a consequence of the presence of a paramagnetic impurity. A non-collinear, tetrahedral arrangement of Mn magnetic moments is locally preferred.

The triple-Q structure is a non-collinear structure but experimentally it has not been possible to distinguish between equally populated 'domains' of single-Q and triple-Q structures. The reason is the fact that the triple-Q state is a *linear* superposition of single-Q states and hence any probe that makes a 'long distance average' measurement will not detect the difference. For magnetic neutron Bragg scattering the magnetic structure factors are identical in the two cases as was first pointed out by Kasper and Kouvel [1].

Since 'long distance average' probes cannot settle the experimental issue of the spin structure, another possibility is to look at short-range or 'local' probes. An application of anisotropy measurements of γ-ray emission from spin polarised ^{54}Mn nuclei in FCC antiferromagnetic $Mn_{72}Ni_{28}$ has been used to distinguish between the single-Q and triple-Q phases and appears to give strong evidence for a triple-Q structure [12]. We will argue that magnetic diffuse scattering may also be considered to be 'local' in character.

Another approach to this problem has been to study the spin-wave spectrum of both single-**Q** and triple-**Q** structures. In principle, mode counting can be used to differentiate between the spin structures [13]. Although this argument has been used in lanthanide systems where spin–orbit coupling is strong, it is not easy to justify it for the present alloy systems. Nevertheless, the magnetic structure of FCC γ-$Fe_{66}Mn_{34}$ has been predicted to be single-**Q** on just these grounds [14, 15]. A Mössbauer transmission study, however, favours a triple-**Q** structure for FCC γ-FeMn alloys [16] in direct contradiction to the spin-wave measurement.

The effects on the magnetic structure of γ-Mn based transition metal alloys have been extensively studied by the magnetic diffuse scattering of neutrons [17, 22]. Neutron Bragg diffraction can only furnish *average* information about the magnetic order, but magnetic diffuse neutron scattering furnishes information about the fluctuations from the average magnetisation. Since an atomic impurity is localised in real space, we might expect that the disturbance induced would also be localised around the dopant site and hence that fluctuations in the magnetisation would depend only on the *local* spin arrangements. Thus, if the spin rearrangement induced by the impurity atoms has a smaller length scale than the size to be expected for magnetic domains, we might expect magnetic diffuse scattering to be a *local* probe of the magnetic structure and as such ought to give evidence for the local spin configuration within a domain. It may therefore be possible to investigate directly the nature of the disturbance of Mn magnetic moments due to the presence of a magnetic or non-magnetic defect. Most of the available data has been analysed within the framework of a model which takes into account a linear superposition of collinear magnetic defects, and whereby a defect increases or decreases the magnitude of Mn moments in its nearest neighbour environments [23]. A model incorporating a precise dependence of the magnetic moments at any site as a function of its magnetic environment has also been applied to available diffuse neutron scattering data on γ-MnNi alloys [24]. In either case there is a large discrepancy between both proposed models and the available data and this suggests that the diffuse magnetic scattering is not due to simple defects in the collinear antiferromagnetic structure.

In this paper, the magnetic diffuse scattering is calculated from the model of the non-collinear defects at first nearest neighbours proposed by Long [11]. The calculated diffuse scatering within the framework of this model, which is virtually parameter free, is compared with the available data from a single crystal of FCC γ-$Mn_{73}Ni_{27}$. The calculated *wavevector dependence* of the diffuse scattering is in good agreement with the measured diffuse scattering, particularly in the [001] direction.

There are several theoretical questions which must be asked before we can make a connection between the diffuse scattering experiments and magnetic structure determination. Firstly, we must find out what information the technique has to offer; whether one can separate out the contributions from different atoms (i.e. if we can determine the spin distortion unambiguously), whether one can deduce the point group symmetry that the impurity has, and what the relationship between Bragg and diffuse scattering is. Only secondly, can we then ask how this information depends on the actual average magnetic moment distribution present. In section 2 we will introduce simple descriptions of how to analyse both Bragg and diffuse scattering and try to find out how to make a connection between diffuse scattering and non-collinear spin fluctuations.

Even if one can find a model spin arrangement for the spin fluctuations which successfully predicts the neutron scattering, there is still an important physical question to consider. What physical phenomena will favour the chosen spin arrangement over the other possible choices? The answer to this question would shed light on the underlying

interactions between the impurities and surrounding moments. In section 3 we will introduce a very simple classical model which will involve Heisenberg interactions between neighbouring spins. We will show that the *ground state* to this problem yields good agreement with the diffuse scattering data for cubic γ-MnNi and that small displacements away from this solution lead quickly to a loss of agreement with the experimentally observed scattering. We are therefore demonstrating that a simple Heisenberg description of the spin interactions predicts the observed diffuse scattering and we suggest that this is a possible description for the underlying physical phenomena at work in the vicinity of the transition metal impurity.

2. Bragg and diffuse scattering from type I FCC antiferromagnets

First we take a look at simple Bragg scattering from commensurate antiferromagnets. This will allow us to represent type I antiferromagnetism with a formalism which is useful for comparing Bragg scattering with diffuse scattering. The electrons which carry the moment in Mn are predominantly in d-orbitals. The spatial extent of these d-orbitals leads to a complication. One gets an 'atomic form factor' decay in the magnetic Bragg scattering corresponding to this uncertainty in position. If we ignore this contribution initially and assume that the spins are perfectly localised on the nuclei, then the spin density on each site may be expanded in terms of Fourier components which define the periodic spatial variations of the magnetism:

$$\boldsymbol{S}(\boldsymbol{R}) = \sum_i \boldsymbol{m}(\boldsymbol{Q}_i)\, \mathrm{e}^{\mathrm{i}\boldsymbol{R}\cdot\boldsymbol{Q}_i}. \tag{2.1}$$

The $\boldsymbol{Q}_i$ is usually a single point, but in frustrated antiferromagnets, we find distinct $\boldsymbol{Q}_i$ which lead classically to degenerate magnetic solutions. This equation therefore describes a *linear* superposition of different magnetic components, the $\boldsymbol{m}(\boldsymbol{Q}_i)$, where each component relates to a distinct point in reciprocal space, the $\boldsymbol{Q}_i$. For the case of type I antiferromagnetism on a FCC lattice, there are three relevant $\boldsymbol{Q}$ points, $\boldsymbol{Q}_1 = (2\pi/a)(1,0,0)$, $\boldsymbol{Q}_2 = (2\pi/a)(0,1,0)$ and $\boldsymbol{Q}_3 = (2\pi/a)(0,0,1)$. The $\boldsymbol{Q}_i$ for type I antiferromagnetism are *commensurate* with the original lattice. The magnetic lattice symmetries are the cubic superlattice corresponding to the four atoms per unit cell experimental description for FCC. The Bragg reflections are found on the reciprocal space cubic lattice generated by the $\boldsymbol{Q}_i$, which includes the nuclear Bragg reflections of the BCC superlattice. The collinear arrangement corresponds to the case where only $\boldsymbol{m}_3$ is non-vanishing and the triple-$\boldsymbol{Q}$ case is that where the three $\boldsymbol{m}$ values are all of equal magnitude and form an orthogonal set.

The Bragg scattering intensity is related to the Fourier transform of the spin density:

$$\boldsymbol{S}(\boldsymbol{K}) = \sum_{\boldsymbol{R}} \boldsymbol{S}(\boldsymbol{R})\, \mathrm{e}^{-\mathrm{i}\boldsymbol{R}\cdot\boldsymbol{K}} = N \sum_i \sum_{\mathrm{G}} \delta(\boldsymbol{K} - \boldsymbol{G} - \boldsymbol{Q}_i)\boldsymbol{m}(\boldsymbol{Q}_i) \tag{2.2}$$

where $\boldsymbol{G}$ is the reciprocal lattice for the original translational symmetry and N is the number of atoms in the crystal.

The most important consequence of assuming that the spins lie at the nuclear positions, is that the Fourier transform of the spin density is *periodic* with the underlying reciprocal space lattice symmetry; in this example BCC. The spin-density information for such a system can be deduced by measuring the relevant scattering in only *one* Brillouin zone. For all our modelling of this problem this contribution to the scattering will be

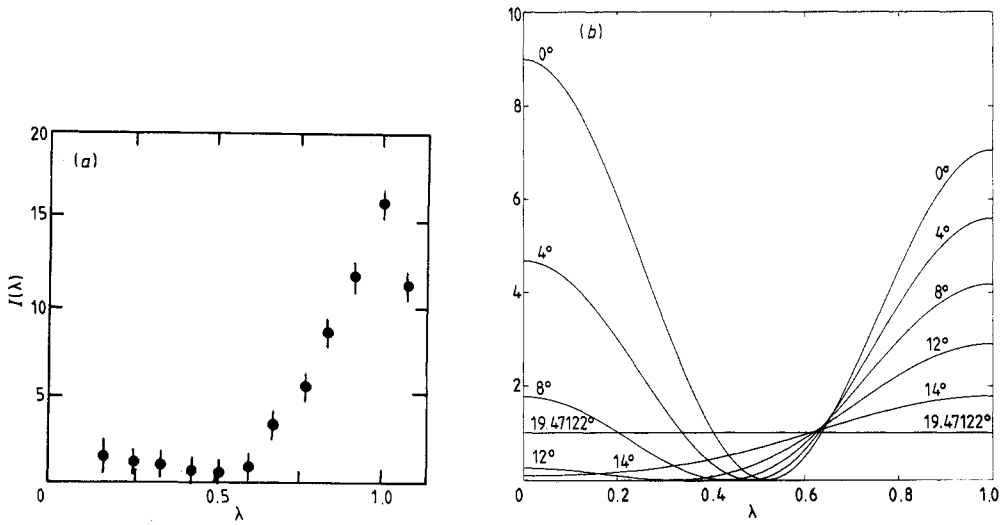

Figure 2. (*a*) The magnetic diffuse scattering from a 'multi-domain' single crystal of $Mn_{73}Ni_{27}$. This data was originally published by Moze and Hicks [22]. We have renormalised the data so that the spatial average of independent, isolated, paramagnetic impurities with all spins localised on the nuclei would yield unit scattering per impurity. The renormalisation includes: a rescaling of 3/2 to compensate for the loss of the parallel spin component, a division by the magnetic form factor to compensate for the spatial extent of the d orbitals, a division by the concentration of impurities and a division by the square of the magnetic moment on the Mn atoms, as deduced by Bragg scattering. usually, extra concentration dependence and short range order factors are included, but we deal with coherence in our own way and therefore do not further renormalise the data. (*b*) The magnetic diffuse scattering intensity from a paramagnetic impurity with a variable shell of 'relaxed' nearest neighbours. The chosen parameters are:

ϕ	$\bar{C}$	I	$\lambda = 0$ $I(1-\bar{C})^2$	$\lambda = 1$ $I(1+\bar{C})^2$
0	−0.061	2.828	9.000	7.059
4	0.044	2.263	4.678	5.589
8	0.212	1.688	1.769	4.182
12	0.542	1.103	0.255	2.895
16	1.599	0.514	0.095	1.783
19.47	∞	0.000	1.000	1.000

periodic. Experimentally, the spatial extent of the d orbitals leads to the atomic form factor complication. This effect is well understood [25] and leads to a slow decay of the scattering from zone to zone. The decay is well described by the Fourier transform of the relevant charge density from an atomic calculation. In order to facilitate our experimental and theoretical comparison, we have extracted the atomic form factor dependence from the *experimental* data (see figure 2).

There is one final important subtlety and this relates to the fact that neutrons can only scatter from magnetic moments *perpendicular* to the direction of the momentum transfer. One finds that the neutron scattering intensity is proportional to [25]:

$$I(\boldsymbol{K}) \propto \boldsymbol{S}^{\perp}(\boldsymbol{K}) \cdot \boldsymbol{S}^{\perp *}(\boldsymbol{K}) \tag{2.3a}$$

$$\boldsymbol{S}^{\perp}(\boldsymbol{K}) = \hat{\boldsymbol{K}} \times (\boldsymbol{S}(\boldsymbol{K}) \times \hat{\boldsymbol{K}}) = \boldsymbol{S}(\boldsymbol{K}) - (\hat{\boldsymbol{K}} \cdot \boldsymbol{S}(\boldsymbol{K}))\hat{\boldsymbol{K}} \tag{2.3b}$$

where $\mathrm{S}^{\perp}(\boldsymbol{K})$ is the component of the spin density perpendicular to the momentum transfer, $\boldsymbol{K}$.

For Bragg scattering we find:

$$I_{\mathrm{Bragg}}(\boldsymbol{K}) \propto \sum_i \sum_{\boldsymbol{G}} \delta(\boldsymbol{K} - \boldsymbol{G} - \boldsymbol{Q}_i)[|\boldsymbol{m}(\boldsymbol{Q}_i)|^2 - |\hat{\boldsymbol{K}} \cdot \boldsymbol{m}(\boldsymbol{Q}_i)|^2] \tag{2.4}$$

and we find the expected Bragg reflections at the magnetic reciprocal lattice vectors. There are two important physical quantities which need to be deduced.

Firstly, there is the actual direction of the spins in real space. If the neutrons scattered isotropically, then the intensity would only depend on the magnitude of the moment and the true spin direction would be unobtainable. It is the fact that neutrons scatter off the perpendicular component of spin which must be used to deduce the moment direction. In practice one looks at the Bragg reflection intensities around the reciprocal lattice and fits the intensities on a shell to $\delta_{\alpha\beta} - \hat{G}_{\alpha}\hat{G}_{\beta}$ for the relevant values of $\boldsymbol{G}$. This procedure is used for each distinct $\boldsymbol{Q}_i$ and the direction of the relevant $\boldsymbol{m}(\boldsymbol{Q}_i)$ is deduced. For the case of FCC Mn, we find that in *all* experimental situations the magnetic moment of each component is parallel to the relevant $\boldsymbol{Q}_i$. This is simple to prove since all one needs to do is to look at the $\boldsymbol{Q}_i$ point and observe that it does not have a Bragg reflection because this vector is parallel to the spin direction of this component.

Secondly, we need to find the relative magnitudes of the distinct, $\boldsymbol{m}(\boldsymbol{Q}_i)$ and whether the state is single-$\boldsymbol{Q}$ or multiple-$\boldsymbol{Q}$. At this stage the structure determination problem emerges. If we had a single domain, then a simple comparison of the intensities at symmetrically related magnetic Bragg reflections would yield the relative magnitudes of the $\boldsymbol{m}(\boldsymbol{Q}_i)$. The most natural magnetic Bragg reflections are $(2\pi/a)(0, 1, 1)$, $(2\pi/a)(1, 0, 1)$ and $(2\pi/a)(1, 1, 0)$, since they are the most intense. The angular variations are optimised since these Bragg vectors are orthogonal to the relevant magnetic components. These Bragg reflections are also second closest to the origin and so optimise the form factor dependence. The only Bragg reflections closer to the origin are the $\boldsymbol{Q}_i$ and these reflections vanish because of the angular factors, a point quite central to the controversy in these materials. Unfortunately, as well as a triple-$\boldsymbol{Q}$ state, three equally populated single-$\boldsymbol{Q}$ domains would yield equal intensity Bragg reflections.

The Bragg reflections are very intense and very sharp, but superimposed on top of the magnetic Bragg spectrum is the magnetic diffuse scattering. This contribution comes from the 'fluctuations' of the spins away from the average, both static and dynamic. In this article we are interested in the static deformations around impurity Ni sites. Since we are considering a disordered alloy, the diffuse scattering is strong and rises as the impurity fraction is increased. In order to facilitate comparison between experiment and theory, we have normalised the scattering by dividing through by the number of impurities present.

The same basic theory covers magnetic diffuse scattering, where now the spins are:

$$\boldsymbol{S}(\boldsymbol{R}) = \sum_i \boldsymbol{m}(\boldsymbol{Q}_i)\, \mathrm{e}^{\mathrm{i}\boldsymbol{R}\cdot\boldsymbol{Q}_i} + \delta\boldsymbol{S}(\boldsymbol{R}) \tag{2.5}$$

and the $\delta\boldsymbol{S}(\boldsymbol{R})$ are the distortions of fluctuations away from the average, which in our case will be localised distortions around Ni impurities. The neutrons still scatter from

the magnetic moments perpendicular to the momentum transfer and the magnetic diffuse contribution is:

$$I_{\text{Diffuse}}(\boldsymbol{K}) \propto \delta \boldsymbol{S}^{\perp}(\boldsymbol{K}) \cdot \delta \boldsymbol{S}^{\perp *}(\boldsymbol{K}) \tag{2.6}$$

which is superimposed on the Bragg contribution, and where the atomic form factor contribution has again been suppressed.

The magnetic diffuse scattering around an impurity is therefore directly related to:

$$\delta \boldsymbol{S}^{\perp}(\boldsymbol{K}) = \hat{\boldsymbol{K}} \times \left(\sum_i \mathrm{e}^{\mathrm{i}\boldsymbol{K}\cdot\boldsymbol{R}_i} \delta \boldsymbol{S}(\boldsymbol{R}_i) \times \hat{\boldsymbol{K}} \right). \tag{2.7}$$

Since the distortions around the impurity are not periodic, the form of $\delta \boldsymbol{S}^{\perp}(\boldsymbol{K})$ is rarely sharp (hence the name diffuse) and the functional dependence of the diffuse scattering *between* the Bragg reflections is the experimental probe of the spin structure. To the extent that the spins are localised on the nuclei (namely the magnetic form factor), the scattering remains periodic in reciprocal space.

As with magnetic Bragg scattering only the magnitude of the $\delta \boldsymbol{S}^{\perp}(\boldsymbol{K})$ can be determined and the loss of the relative phase eliminates any possibility of uniquely determining the distortion. Also analogous to Bragg scattering, much can be deduced from the vanishing of the magnetic diffuse scattering due to the scattering vector being parallel to the spin deformation. Indeed this is the centre of the controversy in γ-MnNi.

The dominant contribution to the magnetic diffuse scattering appears precisely where the missing magnetic Bragg reflections would be. The *spin fluctuations seem to be perpendicular to the spin directions*. We will expend a lot of effort showing that this does not mean that the basic spin structure is necessarily non-collinear as has previously been assumed [26], and in fact we will produce a rather different argument to try to reach this conclusion.

3. A collinear description for the diffuse scattering

It has previously been stated that it is difficult to explain the observed diffuse scattering in cubic γ-MnNi using a collinear defect model [26]. We would like to qualify this claim and replace it with the claim that it is difficult to *believe* in the explanation for the diffuse scattering suggested by the collinear model.

Let us consider a single domain of collinear type I antiferromagnet and assume that there is one impurity atom with a reduced value of the moment. This impurity atom breaks the translational symmetry and most of the spatial point group symmetry. There are certain symmetries that are not *automatically* broken and we will assume that these symmetries are *not* spontaneously broken.

The first unbroken symmetry is the pure spin symmetry associated with rotations about the spin quantisation axis. The arrangement of spins about the impurity can remain collinear. The second set of unbroken symmetries are spatial point group symmetries about the impurity atom. These symmetries map the shells of atoms surrounding the impurity onto themselves. The result is that atoms on the same magnetic sublattice in the same shell of neighbours should have the same moment.

The remaining degrees of freedom consistent with these symmetries are the changes of moment lengths on surrounding shells. If the original moment on the impurity sublattice is $\boldsymbol{S}$ then we may parametrise the new spins by: $(1 + \lambda_n^0)\boldsymbol{S}$ for the spins on the

same sublattice and the nth shell and $-(1+\lambda_n^1)S$ for spins on the other sublattice and the nth shell.

The diffuse neutron scattering from a domain oriented parallel to the x_1 axis and neglecting the explicit form factor dependence is:

$$I_{\text{Diffuse}}(\boldsymbol{K}) = |\delta S_{\boldsymbol{k}}^{\perp}|^2 = (1-\hat{k}_1^2)|\kappa - 1 + \sum_n \lambda_n^0 \gamma_{k0}^n - \sum_n \lambda_n^1 \gamma_{k1}^n|^2 S^2 \qquad (3.1a)$$

where the impurity spin is κS and $\gamma_{k\alpha}^n$ is the relevant structure factor:

$$\gamma_{k\alpha}^n = \sum_{\text{shell}} e^{i\boldsymbol{k}\cdot(\boldsymbol{R}+\boldsymbol{c}_\alpha)} \qquad (3.1b)$$

in terms of the positions of the four atoms in the unit cell, $\boldsymbol{c}_\alpha$.

As has been previously pointed out [27], the contribution at the Bragg reflections $\boldsymbol{Q}_2$ and $\boldsymbol{Q}_3$, corresponding to the other domains, *does not vanish* and indeed could be the source of the observed diffuse scattering in the γ-MnNi alloys.

If we assume that there are three equally populated domains in the cubic crystal, that only the moments on the nearest neighbours of the impurity are disturbed and finally that we will measure parallel to the z axis, then:

$$\tfrac{2}{3}S^2 I(\lambda) = \tfrac{2}{3}S^2 I(\boldsymbol{K}) = |\delta S_{\boldsymbol{k}}^{\perp}|^2 = \tfrac{2}{3}|\kappa - 1 - 4\lambda_1^1 + 4(\lambda_1^0 - \lambda_1^1)\cos\lambda\pi|^2 S^2 \qquad (3.2a)$$

where $\boldsymbol{K} = \lambda \boldsymbol{Q}_3$ and we use λ to describe the spatial dependence in the figures. Using $C = \cos\lambda\pi$ we may parametrise this as:

$$\tfrac{2}{3}S^2 I(\lambda) = \tfrac{2}{3}S^2 I(\boldsymbol{K}) = |\delta S_{\boldsymbol{k}}^{\perp}|^2 = \tfrac{2}{3}S^2 I(\bar{C} - C)^2 \qquad (3.2b)$$

where I is a contribution to the total intensity and $\bar{C}$ parametrises the functional dependence. In figure 2 we have plotted this function for a few values of the parameters.

We have chosen a range of values for $\bar{C}$ and the intensities, I, have been chosen according to the calculations of the next section (see (4.5)) which have an identical functional form. The first observation to make is that the functional form of the observed experimental scattering can only be seen for a very restricted set of values of $\bar{C}$. We need $\bar{C} \sim \frac{1}{2}$ or $\varphi \sim 12°$. The second observation is that the intensity of these calculations is way below that observed. If we take for reference the peak height at [001], then this takes the value $(1 + 4\lambda_1^0)^2$ in this model. In order to get a reasonable fit to experiment, we must allow $\lambda_1^0 \sim 1$ and $\lambda_1^1 \sim 0$. This is precisely the basic content of the fit found by Moze and Hicks [27]. In simple terms, the spins on nearest neighbours with parallel spins *double* in length while the spins on nearest neighbours with antiparallel spins remain virtually unaffected. Extensions to larger clusters in that analysis improved the fit, but did not alter this simple picture.

This scenario seems rather extreme, especially if we consider nearby impurities which, when on the same magnetic sublattice, would elongate the parallel spins even further. If we relax the necessity for the intensities to agree, then the basic functional form of the scattering can also be achieved with $\lambda_1^0 \sim 0.2$ and $\lambda_1^1 \sim -0.1$. This choice ensures that the *sum* of the spins on the nearest neighbours remains constant and is pictured in figure 2 as the curve marked $\varphi = 12°$. Although this assumption is more physically satisfying, we must at some stage seriously consider how to explain the huge surplus intensity at the [001] position, and further explain why near neighbour impurities on different sublattices do not *just cancel out*.

In this model we predict that spins parallel to the lost spin on a paramagnetic impurity grow to compensate for the loss and antiparallel spins shrink also to compensate. This

could be a conclusion, but a more sensible view to take, is to ask whether or not this is physically reasonable and, in addition, what physical phenomena might promote this behaviour.

4. Classical Heisenberg cluster calculations

In this section we focus on the orientations of the spins in the vicinity of an impurity and assume that the lengths of the spins are fixed. The imposed constraints on the lengths of the spins are introduced on physical grounds and ensure a coupling between the three orthogonal spin density waves which is not a simple superposition of linear effects.

If we apply these assumptions to the collinear arrangement of the previous section, then *there is no residual freedom in the system* and the diffuse scattering would be structureless. This is the natural comparison between the single-$\boldsymbol{Q}$ and triple-$\boldsymbol{Q}$ states for our model. The single-$\boldsymbol{Q}$ state yields scattering with no basic reciprocal space dependence, which corresponds precisely to the loss of spin on the impurity atom with all other spins remaining unaffected. This picture has also motivated the *normalisation* of the results we have presented. We present our results with a normalisation for which this featureless impurity state would on average exhibit unit scattering.

The spin structure that is the focus of this section is the triple-$\boldsymbol{Q}$ structure of figure 1(b). The experimental fact, that the tetragonal structural distortion of the weakly doped alloy is lost in the present system, is the main reason for believing that this spin structure might be a more natural starting point than the collinear state. We now proceed to a treatment of impurities in the triple-$\boldsymbol{Q}$ state which is precisely analogous to the development of the last section.

First let us consider the replacement of one spin in the system with an impurity. The impurity breaks most of the symmetries of the system. Translational symmetry is lost and point group symmetries which do not leave the impurity invariant are also broken. The residual symmetry is the point group symmetry about the impurity site. Let us consider the possible orientations of the spins around the impurity which maintain the point group symmetry of the triple-$\boldsymbol{Q}$ spin arrangement in the absence of the impurity.

The point group symmetries map the shells of nearest neighbours onto themselves. We find shells of two types; shells composed of atoms on the same sublattice as the impurity and shells which are composed of equal numbers of atoms from each of the three other sublattices. Point group symmetry suggests first that atoms on the same sublattice which can be mapped onto each other by a pure spatial symmetry should have an identical spin. Secondly combined spin and space rotations about the direction of the spin replaced by the impurity suggest that the spins on the sublattice containing the impurity should have unchanged orientation while the spins on the other sublattices can only be modified by a component of spin parallel to the spin replaced by the impurity.

If we denote the four spin directions in the triple-$\boldsymbol{Q}$ state by $\{\boldsymbol{S}_\alpha;\ \alpha = 0, 1, 2, 3\}$ where the impurity replaces an $\boldsymbol{S}_0$ spin, then the spins in the presence of the impurity may be represented by:

$$\boldsymbol{T}^n_\alpha = \cos\theta_n \boldsymbol{S}_\alpha + \sin\theta_n(3\boldsymbol{S}_0 + \boldsymbol{S}_\alpha)/2\sqrt{2} \tag{4.1a}$$

$$\boldsymbol{T}^n_\alpha = -\sin\varphi_n \boldsymbol{S}_0 + \cos\varphi_n(3\boldsymbol{S}_\alpha + \boldsymbol{S}_0)/2\sqrt{2} \tag{4.1b}$$

for $\alpha = 1, 2, 3$, where n is a label running over the shells of neighbours to the impurity

and the angles θ_n and φ_n are two ways of representing the residual orientational freedom. We have:

$$\boldsymbol{S}_\alpha \cdot \boldsymbol{T}_\alpha^n = S^2 \cos\theta_n \tag{4.2a}$$

$$\boldsymbol{S}_0 \cdot \boldsymbol{T}_\alpha^n = (-1)S^2 \sin\varphi_n \tag{4.2b}$$

and so the physical interpretation of θ_n and φ_n is immediate. θ_n is the angle through which the spin has rotated and φ_n is the angle that the spin makes with the plane perpendicular to $\boldsymbol{S}_0$. If we recall that for the Cu_3Au structure with moments on the Cu sites, the classical ground state finds $\varphi_n = 0$, and so φ_n measures the orientation away from this reference state.

There is no problem in determining the associated diffuse scattering from this type of impurity and we find:

$$\delta\boldsymbol{S}_k = \boldsymbol{S}_0\left[\kappa - 1 + \sum_n\left(\frac{\cos\varphi_n}{2\sqrt{2}} - \sin\varphi_n\right)\gamma_k^n\right] + \sum_\alpha \boldsymbol{S}_\alpha \sum_n\left(\frac{3\cos\varphi_n}{2\sqrt{2}} - 1\right)\gamma_{k\alpha}^n \tag{4.3a}$$

$$\gamma_{k\alpha}^n = \sum_{n-shell} e^{i\boldsymbol{k}\cdot(\boldsymbol{R}+\boldsymbol{c}_\alpha)} \tag{4.3b}$$

$$\gamma_k^n = \sum_{\alpha=1}^{3} \gamma_{k\alpha}^n \tag{4.3c}$$

in terms of the structure factors $\gamma_{k\alpha}^n$, where we only include shells of neighbours not on the impurity sublattice. In section 2 we focussed on the Bragg reflections which vanish because the momentum transfer is parallel to the relevant spin component. If we restrict $\boldsymbol{k}$ in (4.3) to $\boldsymbol{k} = \lambda\boldsymbol{Q}_3$, along the z axis parallel to [001], then:

$$\tfrac{2}{3}S^2 I(\lambda) = \tfrac{2}{3}S^2 I(\boldsymbol{k}) = |\delta\boldsymbol{S}_k^\perp|^2 = \tfrac{2}{3}\left[\kappa - 1 + \sum_n\left(\frac{\cos\varphi_n}{2\sqrt{2}}[\gamma_k^n - 3\gamma_{k3}^n] - \sin\varphi_n\gamma_k^n + \gamma_{k3}^n\right)\right]^2 S^2. \tag{4.4}$$

In figure 2 we restrict attention to nearest neighbours, on the assumption that the impurity disturbance is very short range, and calculate the diffuse scattering as a function of λ for various orientations of the nearest neighbour shell:

$$|\delta\boldsymbol{S}_k^\perp|^2 = \tfrac{2}{3}|\kappa + 3 - 2\sqrt{2}\cos\varphi_1 - 4\sin\varphi_1 + (2\sqrt{2}\cos\varphi_1 - 8\sin\varphi_1)\cos\pi\lambda|^2 S^2. \tag{4.5}$$

The functional dependence of the present triple-$\boldsymbol{Q}$ model is *identical* to that found in the previous section for collinear spins. In fact one can view the present results as a linear superposition of three collinear impurities in the three cartesian directions. The assumption of fixed spin magnitude ensures that *all* the spins compensate for the impurity and we are restricted to *low intensity* scattering. This model can explain the functional form of the scattering but we still need an explanation for the surplus intensity. The observed peak in the diffuse scattering at the magnetic reciprocal lattice vector $\boldsymbol{Q}_3$ (namely $\lambda = 1$) is found for only a small range of angles centred on $\varphi_1 \sim 12°$.

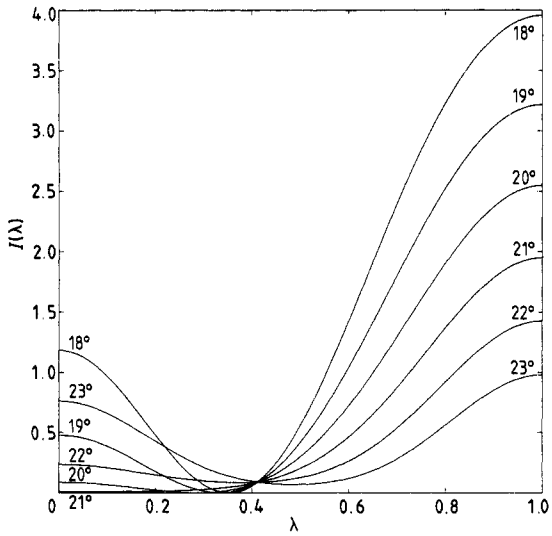

Figure 3. The magnetic diffuse scattering intensity from a paramagnetic impurity with a fixed shell of 'relaxed' nearest neighbours and a variable shell of 'relaxed' next nearest relevant neighbours. The chosen parameters are:

ϕ_1	ϕ_2	$\lambda = 0$	$\lambda = 1$
12	18	1.185	3.958
12	19	0.478	3.220
12	20	0.088	2.550
12	21	0.009	1.951
12	22	0.236	1.427
12	23	0.761	0.980

The second shell of neighbours is unmoved when $\phi_2 = 19.47122°$.

In figure 3 we fix the nearest neighbour orientation and allow the next nearest *relevant* shell of neighbours to move. The peak sharpens when the next shell of neighbours rotates in the *opposite* direction to the first shell but at the same time the intensity drops quite sharply.

So far we have considered the orientations of the spins surrounding the impurity which best match the magnetic diffuse scattering near the magnetic Bragg reflections in γ-MnNi alloys. Now let us consider which physical phenomena might induce these particular spin orientations. In a recent article, classical Heisenberg energies were used to predict the orientation of the spins in a cluster surrounding an impurity [11]. Let us see what this model predicts for the magnetic diffuse scattering.

We consider a cluster of spins around the impurity which are allowed to relax while the remainder of the spins remain in the triple-**Q** spin configuration. The cluster of spins relaxes in such a way as to minimise the classical Heisenberg energy with nearest neighbour antiferromagnetic exchange. The calculational details are given in the appendix and we give the results for when the nearest neighbour shell and first two relevant shells are allowed to relax in figures 4(*b*) and 4(*c*) respectively as a function of the impurity spin magnitude.

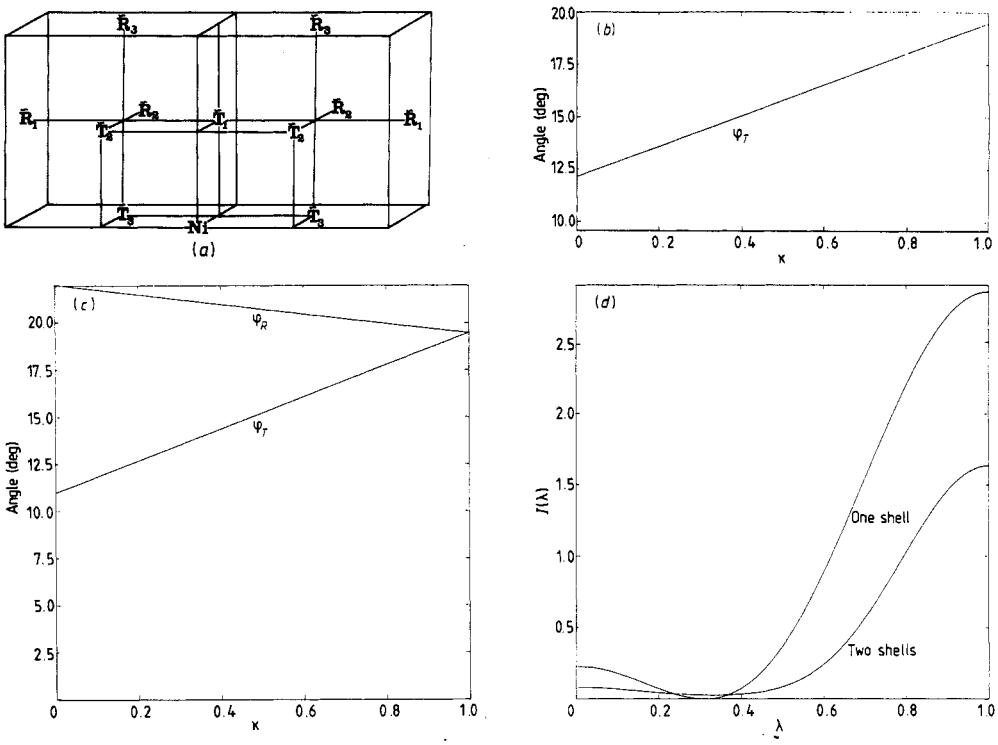

Figure 4. (*a*) The atomic positions of the first and second shells of relevant neighbours to the Ni impurity. (*b*) The angle that the nearest neighbour spins rotate as a function of the impurity length reduction, κ, when they minimise the classical Heisenberg energy. (*c*) The angles that the first two neighbouring shells rotate as a function of the impurity length reduction, κ, when they minimise the classical Heisenberg energy. (*d*) The magnetic diffuse scattering intensity from the Heisenberg relaxed impurity calculations.

For both calculations the nearest neighbour shell is oriented in such a way as to yield the large peak at the [001] position (figure 4(*d*)). The nearest neighbour shell moves so as to compensate locally for the impurity spin. When the next shell is allowed to relax, we find that the shell of nearest neighbours *overcompensates* for the impurity spin and the outer shell cancels off this extra contribution by moving a small angle in the opposite direction.

The cluster calculations so far presented have been for very short range interactions between spins and very dilute impurities. There is no direct evidence contradicting the assumption that the spin–spin interactions are short range, but the assumption that the impurities are dilute is very dubious. In the γ-MnNi alloys the cubic phase is only observed at a doping level of more than about 20% Ni in Mn. It was argued in our previous work that the doping of paramagnetic impurities *drives* a collinear phase into a non-collinear phase but that macroscopic doping is required. In order to analyse the likely effects of stronger concentrations of impurities, we look at a pair of nearby impurities. There is evidence of short range order between Ni atoms, there being a higher probability of finding two Ni atoms on cube diagonals [22, 27]. We therefore study the case of two impurity spins at positions **0** and $a(1, 1, 1)$.

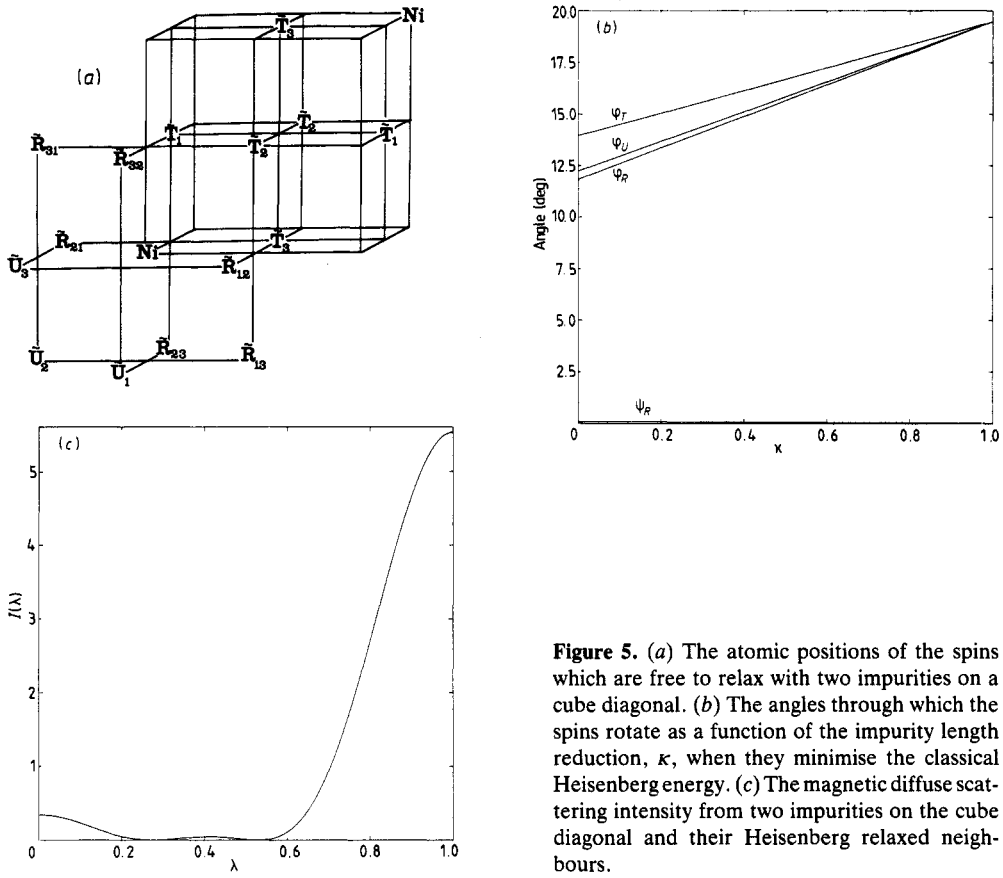

Figure 5. (*a*) The atomic positions of the spins which are free to relax with two impurities on a cube diagonal. (*b*) The angles through which the spins rotate as a function of the impurity length reduction, κ, when they minimise the classical Heisenberg energy. (*c*) The magnetic diffuse scattering intensity from two impurities on the cube diagonal and their Heisenberg relaxed neighbours.

The symmetry consistent with these impurities is shown in figure 5(*a*) where:

$$\boldsymbol{T}_\alpha = -\sin\varphi_T \boldsymbol{S}_0 + \cos\varphi_T(3\boldsymbol{S}_\alpha + \boldsymbol{S}_0)/2\sqrt{2} \tag{4.6a}$$

$$\boldsymbol{R}_{\alpha\beta} = -\sin\varphi_R \boldsymbol{S}_0 - (\cos\varphi_R/2\sqrt{2})[\cos\psi_R(2\boldsymbol{S}_0 + 3\boldsymbol{S}_\alpha + 3\boldsymbol{S}_\beta) - \sqrt{3}\sin\psi_R(\boldsymbol{S}_\beta - \boldsymbol{S}_\alpha)] \tag{4.6b}$$

$$\boldsymbol{U}_\alpha = -\sin\varphi_U \boldsymbol{S}_0 + \cos\varphi_U(3\boldsymbol{S}_\alpha + \boldsymbol{S}_0)2\sqrt{2} \tag{4.6c}$$

in terms of the three angles $\boldsymbol{S}_0 \cdot \boldsymbol{X} = (-1)S^2 \sin\varphi_X$ and the angle ψ_R which is the angle through which the spin has rotated away from the plane containing the original spin and the impurity spin. We show how to determine the lowest energy in the appendix and give the result in figure 5(*b*). The angles that the spins rotate are *very* similar to the single impurity case, where the only complication is that the spins *between* the two impurities do not rotate as far as the single impurity calculation suggests. This result shows that simple naïve additive arguments cannot be trusted, because nearest neighbours and next nearest neighbours rotate in opposite directions and the topology means that some atoms fulfill both roles. The symmetry breaking rotations ψ_R are very small in all cases.

When we analyse the diffuse scattering from this cluster we discover several facts. Firstly the functional form of the experimental scattering is reproduced as with the single-

impurity calculations. Secondly and much more important, the intensity of the magnetic diffuse scattering is greatly enhanced. If we compare the calculation of one impurity presented in figure 4(*d*) with the present result in figure 5(*c*), then we find an increase in the scattering *per impurity atom* of a factor of *two*. The simple corrections of the Marshall model [23] would predict a *reduction* in intensity because some of the contributing host atoms are replaced by impurities (in fact the factors $(1 - c)$ where c is the concentration of impurities in that analysis are attributable to this source). The source of the extra scattering intensity is easily understood. In the Marshall model the impurities are assumed independent and so a linear superposition of the *scattering intensity* is assumed. In our model the two impurities are *coherent* and the *moment fluctuations* are additive with the intensity behaving as the *square* of the moments. This is the source of the surplus intensity at the [001] position.

The final important question to consider is whether the effects of two nearby impurities will cancel or not. In the previous calculation all the host atoms were nearest neighbours to at most one impurity atom and the resulting behaviour is well described by two *coherently* superimposed single impurity distortions. Our final cluster depicted in figure 6(*a*) finds host atoms with *two* nearest neighbour impurities. The calculation is presented in the appendix and the resulting spin distortions which are represented by:

$$\boldsymbol{T}_1 = -\sin\varphi_T \boldsymbol{S}_0 + (\cos\varphi_T/2\sqrt{2})[\cos\psi_T(3\boldsymbol{S}_1 + \boldsymbol{S}_0) + \sqrt{3}\sin\psi_T(\boldsymbol{S}_3 - \boldsymbol{S}_2)] \quad (4.7a)$$

$$\boldsymbol{R}_3 = -\sin\varphi_R \boldsymbol{S}_0 + (\cos\varphi_R/2\sqrt{2})(3\boldsymbol{S}_3 + \boldsymbol{S}_0) \quad (4.7b)$$

$$\boldsymbol{U}_1 = -\sin\varphi_U \boldsymbol{S}_0 + (\cos\varphi_U/2\sqrt{2})[\cos\psi_U(3\boldsymbol{S}_1 + \boldsymbol{S}_0) + \sqrt{3}\sin\psi_U(\boldsymbol{S}_3 - \boldsymbol{S}_2)] \quad (4.7c)$$

are pictured in figure 6(*b*). Although the two angles ψ_T and ψ_U remain small, the three φ_X are rather different from the previous calculations. The dominant effect is that the spins with two impurity neighbours flop down into the Cu_3Au directions. This is a non-linear effect there being almost three times as big a rotation as for the single impurity case. Interestingly the $\boldsymbol{R}_3$ spins hardly move at all and the $\boldsymbol{U}_{1(2)}$ spins rotate further than for one impurity.

When we come to the resulting magnetic diffuse scattering, the reduction in symmetry for this cluster yields rather different contributions in the three cartesian directions. The results are depicted in figure 6(*c*). When the scattering vector is parallel to the vector joining the impurities we find a hugely enhanced contribution which has half the experimentally observed intensity, and perpendicular to that direction we find similar scattering to that for the single impurity case. There is *no* reduction in the intensity averaged over the three cartesian directions when compared with the more distant impurities.

5. Conclusions

If we assume that the Ni atoms are effectively paramagnetic, then we have a parameter free description of the magnetic diffuse scattering as a function of impurity positions. The basic theoretical assumptions are:

(i) host atom spins have fixed magnitude;

(ii) spatial symmetries of the system which remain in the presence of the impurities are not spontaneously broken;

(iii) the host spins interact with nearest neighbour Heisenberg interactions.

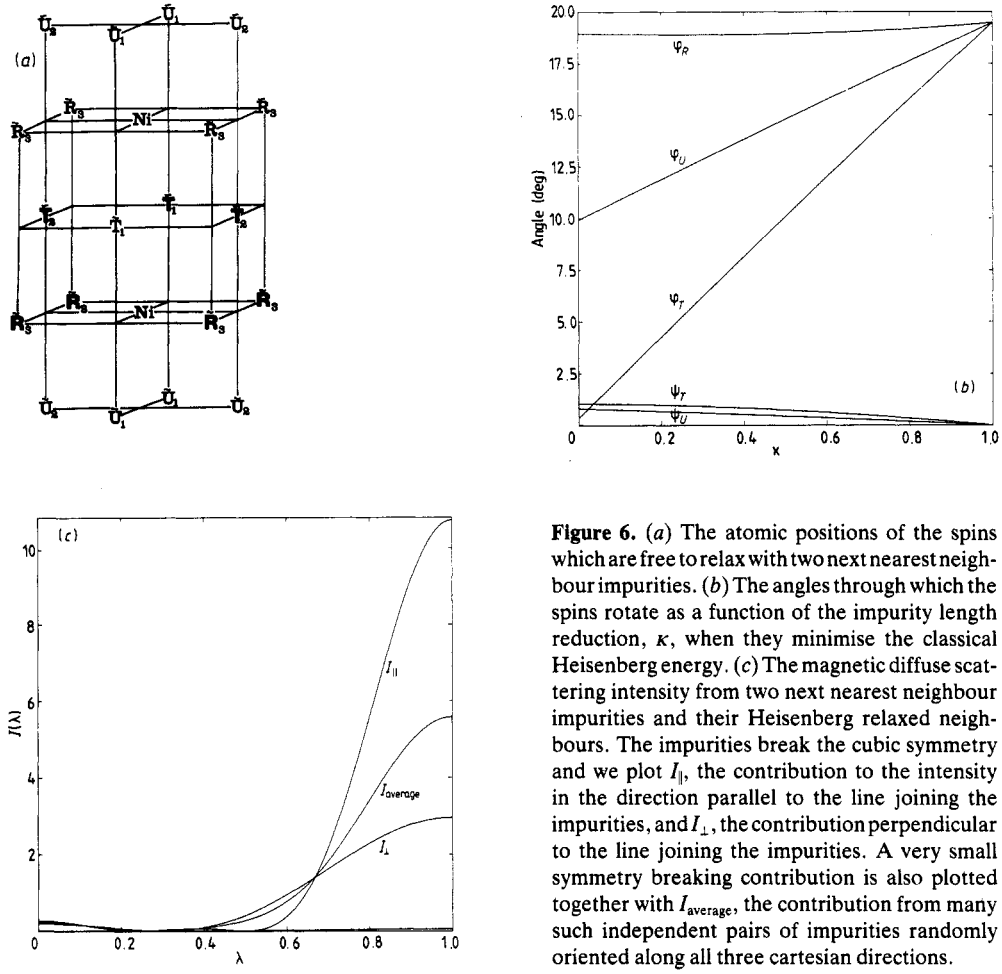

Figure 6. (*a*) The atomic positions of the spins which are free to relax with two next nearest neighbour impurities. (*b*) The angles through which the spins rotate as a function of the impurity length reduction, κ, when they minimise the classical Heisenberg energy. (*c*) The magnetic diffuse scattering intensity from two next nearest neighbour impurities and their Heisenberg relaxed neighbours. The impurities break the cubic symmetry and we plot $I_{\parallel}$, the contribution to the intensity in the direction parallel to the line joining the impurities, and $I_{\perp}$, the contribution perpendicular to the line joining the impurities. A very small symmetry breaking contribution is also plotted together with $I_{average}$, the contribution from many such independent pairs of impurities randomly oriented along all three cartesian directions.

Under these assumptions a collinear impurity would yield completely structureless magnetic diffuse scattering. Impurities in the triple-**Q** state, however, yield precisely the experimentally observed functional form of magnetic diffuse scattering.

If the comparison is extended to correlated impurities, then for the non-collinear state the spins between the impurities perform the augmented rotations suggested in section 4. For the collinear state, none of the host spins would be expected to move. The expected correlated scattering can be deduced from the *nuclear diffuse scattering*, which also only depends on the positions of the impurity atoms. Experimentally there is no real comparison between the two as is exhibited in the work of Moze and Hicks [22]. Only if the magnitudes of the host spins are allowed to fluctuate is there any hope of using the collinear state to explain the magnetic diffuse scattering.

If we relax our assumption that the spins are of fixed magnitude, then the collinear impurity can also describe the functional form of the scattering. The basic problem with the collinear description, is that in order to achieve the enormous *intensity* of scattering the local spin distortions are required to be huge with neighbouring spins *doubling* in magnitude. Even more disturbing is that when impurities are close together, simple

arguments would suggest that their effects would *cancel* making the huge scattering intensity even harder to predict.

Both of these problems are avoided in our description. The physical picture our model suggests is small rotations of the host spins locally compensating for the impurity atoms. When impurity atoms are close together, rather than cancel, we find that the enhanced stability of the nearby Cu_3Au spin structure tends to non-linearly *increase* the local distortion rather than reducing it. Both of these predictions are more satisfying than their collinear counterparts.

Another important consideration is that for the triple-$\boldsymbol{Q}$ state whatever the local symmetry of the impurities, there is *always* a direction in spin space in which the host spins can relax and compensate for the impurities.

One of the most important observations that we make is that the huge intensity at the [001] position can be explained by local *coherence* between neighbouring impurities. This local coherence probably becomes lost in the *orientational* nature of the local impurity symmetries which can be used to explain why long range phase coherence does not result. In fact the experimentally observed intensity is found in the scattering enhancement of around five coherent impurities since the intensity per impurity scales linearly with the number of coherently coupled impurities. The most effective scattering centres have two impurities which are parallel to the scattering vector as depicted in figure 6(a, c).

The assumption of a very short range interaction between spins gives remarkably good agreement with experiment and we take this to indicate that this model is fundamentally describing the basic physical processes at work in this system.

Finally we would like to point out the physical reason for the huge peak at [001] in our model. The FCC lattice is antiferromagnetically frustrated. The ordering produces scattering at the [001] Bragg reflections. Since each atom finds only eight antiparallel neighbours with four parallel neighbours the ordering yields only *one third* of the unfrustrated maximum. The inclusion of Nickel impurities allows a local release of the frustration and a corresponding enhancement of the Néel ordering. This is the physical source of the extra scattering at [001].

Appendix

The classical solution to the Heisenberg model finds the spins parallel to the field made by the nearest neighbours. For the single impurity we find:

$$\lambda_T \boldsymbol{T}_\alpha = \kappa \boldsymbol{S}_0 + 3\boldsymbol{S}_0 + 2\boldsymbol{T}_\beta + 2\boldsymbol{T}_\gamma + 2\boldsymbol{R}_\beta + 2\boldsymbol{R}_\gamma \tag{A1}$$

with $\{\alpha, \beta, \gamma\} = \{1, 2, 3\}$ for the nearest neighbours and:

$$\lambda_R \boldsymbol{R}_\alpha = 4\boldsymbol{S}_0 + 2\boldsymbol{S}_\beta + 2\boldsymbol{S}_\gamma + \boldsymbol{T}_\beta + \boldsymbol{T}_\gamma + \boldsymbol{R}_\beta + \boldsymbol{R}_\gamma \tag{A2}$$

for the next relevant shell of neighbours. The parameters λ_T and λ_R are Lagrange multipliers which are chosen so that $\boldsymbol{T}_\alpha$ and $\boldsymbol{R}_\alpha$ are correctly normalised.

The nearest neighbour solution is that to (A1) where $\boldsymbol{R}_\alpha = \boldsymbol{S}_\alpha$ and the calculation where both neighbouring shells are free to move is the solution to (A1) and simultaneously to (A2).

The best technique to find the solution is to define a new basis:

$$\begin{bmatrix} X' \\ X \\ X^* \end{bmatrix} = \frac{1}{\sqrt{3}} \begin{bmatrix} 1 & 1 & 1 \\ 1 & \omega & \omega^2 \\ 1 & \omega^2 & \omega \end{bmatrix} \begin{bmatrix} X_1 \\ X_2 \\ X_3 \end{bmatrix} \tag{A3}$$

for which the equations separate to become:

$$\begin{bmatrix} 4-\lambda_T & 4 \\ 2 & 2-\lambda_R \end{bmatrix} \begin{bmatrix} T' \\ R' \end{bmatrix} = \begin{bmatrix} -(3+\kappa)\sqrt{3}S_0 \\ 2S' - 2\sqrt{3}S_0 \end{bmatrix}$$

$$\begin{bmatrix} 2+\lambda_T & 2 \\ 1 & 1+\lambda_R \end{bmatrix} \begin{bmatrix} T \\ R \end{bmatrix} = \begin{bmatrix} 0 \\ -2S \end{bmatrix} \tag{A4}$$

and these are straightforward linear equations. Noting that $\sqrt{3}S' = -S_0$, we may deduce φ_X by observing that $X' = (-1)\sqrt{3}S_0 \sin \varphi_X$. It only remains to choose λ_T and λ_R by normalisation.

The calculation with two impurities on the cube diagonal is also very similar and we find:

$$\lambda_T T_\alpha = \kappa S_0 + 3S_0 + S_\beta + S_\gamma + 2T_\beta + 2T_\gamma + R_{\beta\alpha} + R_{\gamma\alpha} \tag{A5}$$

$$\lambda_R R_{\beta\gamma} = \kappa S_0 + 3S_0 + 2S_\beta + 2S_\gamma + T_\gamma + R_{\beta\alpha} + R_{\alpha\gamma} + U_\beta \tag{A6}$$

$$\lambda_U U_\alpha = \kappa S_0 + 3S_0 + 2S_\beta + 2S_\gamma + R_{\alpha\beta} + R_{\alpha\gamma} + U_\beta + U_\gamma. \tag{A7}$$

The change of basis technique is still useful but now we employ $\{R', R, R^*\}$ for $\{R_{23}, R_{31}, R_{12}\}$ and $[r', r, r^*]$ for $\{R_{32}, R_{13}, R_{21}\}$. The transformed equations become:

$$\begin{bmatrix} 4-\lambda_T & 1 & 0 & \\ 1 & -\lambda_R & 1 & \\ 1 & 2 & 1 & \\ 0 & 1 & 2-\lambda_U & \end{bmatrix} \begin{bmatrix} T' \\ R' \\ r' \\ U' \end{bmatrix} = \begin{bmatrix} -2S' - (3+\kappa)\sqrt{3}S_0 \\ -4S' - (3+\kappa)\sqrt{3}S_0 \\ -4S' - (3+\kappa)\sqrt{3}S_0 \\ -4S' - (3+\kappa)\sqrt{3}S_0 \end{bmatrix} \tag{A8}$$

$$\begin{bmatrix} 2+\lambda_T & -\omega^2 & -\omega & 0 \\ -\omega & \lambda_R & 1 & -\omega^2 \\ -\omega^2 & 1 & \lambda_R & -\omega \\ 0 & -\omega & -\omega^2 & 1+\lambda_U \end{bmatrix} \begin{bmatrix} T \\ R \\ r \\ U \end{bmatrix} = \begin{bmatrix} -S \\ -2S \\ -2S \\ -2S \end{bmatrix} \tag{A9}$$

and we are left to solve and normalise.

The final calculation with next nearest neighbour impurities yields:

$$\lambda_T T_1 = 2(1+\kappa)S_0 + 2S_2 + 2T_2 + 4R_3 \tag{A10}$$

$$\lambda_T T_2 = 2(1+\kappa)S_0 + 2S_1 + 2T_1 + 4R_3 \tag{A11}$$

$$\lambda_R R_3 = (3+\kappa)S_0 + 2S_1 + T_1 + U_1 + 2S_2 + T_2 + U_2 \tag{A12}$$

$$\lambda_U U_1 = (3+\kappa)S_0 + 2S_2 + 2U_2 + 2S_3 + 2R_3 \tag{A13}$$

$$\lambda_U \boldsymbol{U}_2 = (3 + \kappa)\boldsymbol{S}_0 + 2\boldsymbol{S}_1 + 2\boldsymbol{U}_1 + 2\boldsymbol{S}_3 + 2\boldsymbol{R}_3. \tag{A14}$$

This cluster has reduced symmetry to previous cases and:

$$\begin{bmatrix} 2-\lambda_T & 8 & 0 \\ 1 & -\lambda_R & 1 \\ 0 & 4 & 2-\lambda_U \end{bmatrix} \begin{bmatrix} \boldsymbol{T}_1 + \boldsymbol{T}_2 \\ \boldsymbol{R}_3 \\ \boldsymbol{U}_1 + \boldsymbol{U}_2 \end{bmatrix} = \begin{bmatrix} 2\boldsymbol{S}_3 - 2(1+2\kappa)\boldsymbol{S}_0 \\ 2\boldsymbol{S}_3 - (1+\kappa)\boldsymbol{S}_0 \\ 2\boldsymbol{S}_3 - 2(2+\kappa)\boldsymbol{S}_0 \end{bmatrix} \tag{A15}$$

$$\boldsymbol{T}_1 - \boldsymbol{T}_2 = (2/2 + \lambda_T)(\boldsymbol{S}_2 - \boldsymbol{S}_1) \tag{A16}$$

$$\boldsymbol{U}_1 - \boldsymbol{U}_2 = (2/2 + \lambda_U)(\boldsymbol{S}_2 - \boldsymbol{S}_1) \tag{A17}$$

and we are left to solve and normalise.

References

[1] Kouvel J S and Kasper J S 1963 *J. Phys. Chem. Solids* **24** 529
[2] Cade N A 1980 *J. Phys. F: Met. Phys.* **10** L187
[3] Cade N A and Young W 1977 *Adv. Phys.* **26** 393
[4] Cade N A and Young W 1980 *J. Phys. F: Met. Phys.* **10** 2035
[5] Jo T 1983 *J. Phys. F: Met. Phys.* **13** L211
[6] Hirai K and Jo T 1985 *J. Phys. Soc. Japan* **54** 3567
[7] Jo T and Hirai K 1984 *J. Phys. Soc. Japan* **53** 3183
[8] Sato H and Maki K 1976 *Prog. Theor. Phys.* **55** 319
[9] Kubler J, Hock K H, Sticht J and Williams A R 1988 *J. Appl. Phys.* **63** 3482
[10] Henley C L 1989 *Phys. Rev. Lett.* **62** 2056
[11] Long M W 1989 *J. Phys.: Condens. Matter* **1** 2857
[12] Kawarazaki S, Fujita K, Yasuda K, Sasaki Y, Mizusaki T and Hirai A 1988 *Phys. Rev. Lett.* **61** 471
[13] Jensen J and Bak P 1981 *Phys. Rev.* B **23** 6180
[14] Bisanti P, Mazzone G and Sacchetti F 1987 *J. Phys. F: Met. Phys.* **17** 1425
[15] Tajima K, Ishikawa Y, Endoh Y and Noda Y 1976 *J. Phys. Soc. Japan* **41** 1195
[16] Kennedy S J and Hicks T J 1987 *J. Phys. F: Met. Phys.* **17** 1599
[17] Davis J R and Hicks T J 1977 *J. Phys. F: Met. Phys.* **7** 2153
[18] Cywinski R, Wells P, Campbell S J and Hicks T J 1980 *Nukleonika* **25** 787
[19] Gibbs P, Moze O and Hicks T J 1981 *J. Phys. F: Met. Phys.* **11** L83
[20] Moze O and Hicks T J 1979 *J. Magn. Magn. Mater.* **14** 250
[21] Moze O and Hicks T J 1981 *J. Phys. F: Met. Phys.* **11** 1471
[22] Moze O and Hicks T J 1982 *J. Phys. F: Met. Phys.* **12** 1
[23] Marshall W 1968 *J. Phys. C: Solid State Phys.* **1** 88
[24] Hicks T J 1977 *J. Phys. F: Met. Phys.* **7** 481
[25] Lovesey S W 1984 *Theory of Neutron Scattering from Condensed Matter* vol 2 (Oxford: Clarendon)
[26] Rainford B D 1982 *J. Physique* suppl 12 **43** 7
[27] Moze O and Hicks T J 1984 *J. Phys. F: Met. Phys.* **14** 211
[28] Moze O and Hicks T J 1984 *J. Phys. F: Met. Phys.* **14** 221